Erratum

Liu, J., Chau, C.-H., Liu, H., Jang, B. R., Li, X., Chan, Y.-S. and Shum, D. K. Y. (2006). Upregulation of chondroitin 6-sulphotransferase-1 facilitates Schwann cell migration during axonal growth. *J. Cell Sci.* **119**, 933-942.

We apologise for an error in the first name of Y.-S. Chan, which should be Ying-Shing not Ying-Shang.

The error appeared in both the print and online versions of this article.

Upregulation of chondroitin 6-sulphotransferase-1 facilitates Schwann cell migration during axonal growth

Jun Liu[1], Chi-Ho Chau[1,2], Hengying Liu[1], Benjamin R. Jang[1], Xiaoguang Li[1,3], Ying-Shang Chan[2] and Daisy K. Y. Shum[1,*]

[1]Department of Biochemistry and [2]Department of Physiology, Faculty of Medicine, The University of Hong Kong, 21 Sassoon Road, Pokfulam, Hong Kong, China
[3]Department of Neurology, Peking Union Medical College Hospital, Beijing, China
*Author for correspondence (e-mail: shumdkhk@hkucc.hku.hk)

Accepted 15 November 2005
Journal of Cell Science 119, 933-942 Published by The Company of Biologists 2006
doi:10.1242/jcs.02796

Summary

Cell migration is central to development and post-traumatic regeneration. The differential increase in 6-sulphated chondroitins during axonal growth in both crushed sciatic nerves and brain development suggests that chondroitin 6-sulphotransferase-1 (C6ST-1) is a key enzyme that mediates cell migration in the process. We have cloned the cDNA of the C6ST-1 gene (*C6st1*) (GenBank accession number AF178689) from crushed sciatic nerves of adult rats and produced ribonucleotide probes accordingly to track signs of 6-sulphated chondroitins at the site of injury. We found *C6st1* mRNA expression in Schwann cells emigrating from explants of both sciatic nerve segments and embryonic dorsal root ganglia. Immunocytochemistry indicated pericellular 6-sulphated chondroitin products around C6ST-1-expressing frontier cells. Motility analysis of frontier cells in cultures subjected to staged treatment with chondroitinase ABC indicated that freshly produced 6-sulphated chondroitin moieties facilitated Schwann cell motility, unlike restrictions resulting from proteoglycan interaction with matrix components. Sciatic nerve crush provided further evidence of in vivo upregulation of the C6ST-1 gene in mobile Schwann cells that guided axonal regrowth 1-14 days post crush; downregulation then accompanied declining mobility of Schwann cells as they engaged in the myelination of re-growing axons. These findings are the first to identify upregulated *C6st1* gene expression correlating with the motility of Schwann cells that guide growing axons through both developmental and injured environments.

Supplementary material available online at
http://jcs.biologists.org/cgi/content/full/119/5/933/DC1

Key words: Chondroitin sulphate proteoglycans, Development, Dorsal root ganglion, Sciatic nerve crush, Nerve regeneration

Introduction

Cell migration is central to development and post-traumatic regeneration. Tuning of the pericellular environment is required to achieve optimum adhesiveness for the mobile phenotype. The increased chondroitin sulphate proteoglycans (CSPGs) reported in injured neural environments of adult mammals (Braunewell et al., 1995; Shum and Chau, 1996; Sandvig et al., 2004; Silver and Miller, 2004) suggest contribution to this effect. This is reinforced by in vitro studies which demonstrated expression of pericellular CSPGs as a requirement for invasive migration into a fibrin matrix (Henke et al., 1996; Clarke et al., 2004). The multiplicity of core proteins of CSPGs and the heterogeneity of chondroitin sulphate substitutions to the core have confounded attempts to distinguish forms that facilitate cell migration in vivo. The distinctive increases in 6-sulphated chondroitins during axonal regrowth in crushed sciatic nerves (Chau and Shum, 1997; Liu et al., 2001) and in brain development (Fernaud-Espinosa et al., 1996; Kitagawa et al., 1997; Properzi et al., 2005) however highlight 6-sulphation of chondroitins as a key step that the migrant cell exploits to tune its pericellular environment.

The sulphation of chondroitins is catalyzed by chondroitin 6-sulphotransferase (C6ST), chondroitin 4-sulphotransferase and uronyl 2-sulphotransferase (Habuchi, 2000; Fukuda et al., 2001). Differential sulphation is thought to depend on correct juxtaposition of the relevant sulphotransferase(s) and the acceptor chondroitin domain within a subcompartment of the Golgi network (Prydz and Dalen, 2000; Silbert and Sugumaran, 2002). In animals that develop normally, there is little reason to suggest defects of these proteins or their colocalisation in time and space. The distinctive increase in 6-*O*-sulphated isomers of chondroitin sulphate in the injured environment (Chau and Shum, 1997) could therefore be a consequence of stimulated expression of the C6ST gene.

Molecular cloning of human C6ST revealed two orthologous genes, *C6ST-1* (Fukuta et al., 1995; Fukuta et al., 1998; Uchimura et al., 1998) and *C6ST-2* (Kitagawa et al., 2000). Expression of both isoforms in the brain was evident during development but negligible in the adult. Attempts to pursue functional analysis in vivo with mice deficient in the *C6st1* gene found no apparent abnormality in brain development (Uchimura et al., 2002), suggesting possible redundancy among the C6ST isoforms. By contrast, glial cells in the lesioned rat brain were found to upregulate *C6st1* expression

(Properzi et al., 2005). Studies with cell cultures found that matrix-bound proteoglycans bearing 2,6- or 4,6-bissulphated chondroitin sulphate disaccharide repeats possessed neurite-outgrowth-promoting properties by virtue of their affinity for such factors as fibroblast growth factors, pleiotrophin and midkine (Clement et al., 1998; Deepa et al., 2002). Growth factors that are bound to CSPGs could be competed out by 6-sulphated chondroitins but not by 4-sulphated chondroitins. Variations in sulphation of chondroitin sulphate glycoforms can therefore fine-tune bio-availability of growth factors to sprouting neurites.

For Schwann cells to support axonal regrowth, they assume a mobile phenotype to catch up with regenerating sprouts that emerge and extend within hours from the nodes of Ranvier proximal to the site of injury (Torigoe et al., 1996; Tseng et al., 2003). Direct evidence of Schwann cell migration along axons in vivo has recently been shown against the transparency of zebrafish embryos and ErbB signaling was suggested as a requirement for directed migration of the cells (Lyons et al., 2005). Motile machinery and directive signaling aside, we hypothesise that migrating Schwann cells upregulate expression of C6ST genes to produce pericellular 6-sulphated chondroitin moieties that function in counteracting cell adhesiveness of the substrate. We exploited explants of embryonic dorsal root ganglia (DRG) to study both leading and lagging Schwann cells in relation to developing neurites in vitro. *C6st1* expression was identifiable in leading Schwann cells that made frequent and transient contacts with developing neurites; this contrasted with the undetectable expression in lagging Schwann cells that remained associated with axon fascicles. We also used sciatic nerve crush to provide a regenerative environment for the study of mobile Schwann cells in relation to regrowing axons in vivo. *C6st1* expression was upregulated in Schwann cells that became mobile at early stages post crush, ahead of regrowing axons. Schwann cells that resumed the myelinating phenotype downregulated *C6st1* expression. Our results are the first to suggest that 6-sulphated chondroitin moieties are produced to facilitate Schwann cell migration during axonal growth.

Results

Rat *C6st1* shows sequence homology to the mouse and human gene

Following the discovery of increased water-soluble 6-sulphated chondroitin isoforms in the crushed sciatic nerve, we recovered RNA from crushed nerves and used it to identify and clone the cDNA of rat *C6st1* (Fig. 1A). From the nucleotide sequence of the cloned cDNA, the amino acid sequence of the protein was deduced (supplementary material Fig. S1A). The hydropathy plot reveals a hydrophobic stretch of 19 residues towards the N-terminus (supplementary material Fig. S1B), predicting a type II transmembrane domain that is common to many Golgi-associated sulphotransferases and glycosyltransferases. In addition, the six N-linked glycosylation sites predicted in the rat sequence (supplementary material Fig. S1A) correspond to those found in the mouse and human sequences.

The amino acid sequence of the rat C6ST-1 indicated 87, 93 and 74% identity to the reported sequences of the human, mouse, and chick C6ST-1, respectively (supplementary material Fig. S1C). Within the regions of conserved amino acids, motifs for the binding of 5′-phosphosulphate and the 3′-phosphate components (supplementary material Fig. S1C) of the activated sulphate donor, PAPS, could be located.

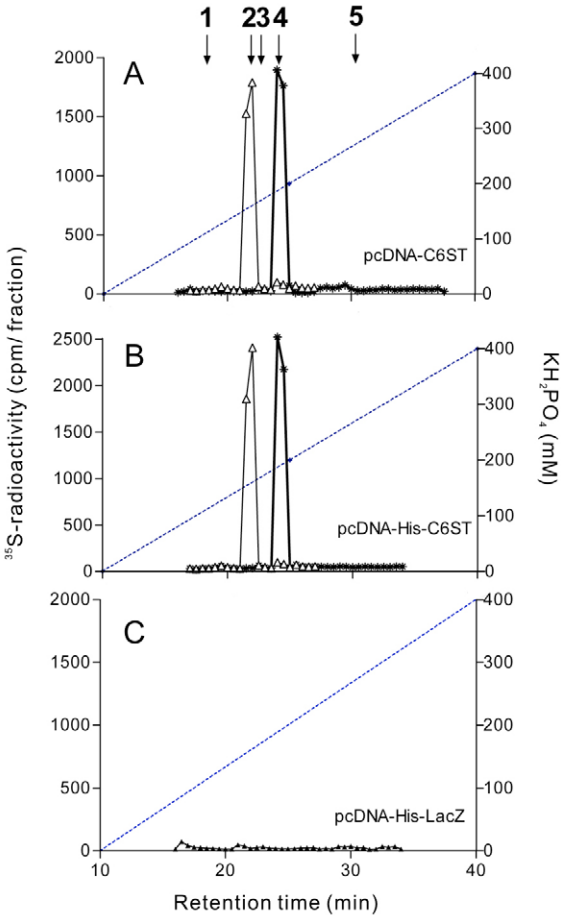

Fig. 1. Recombinant rat C6ST-1 catalyzes sulphation of chondroitin at C-6 of GalNAc residues. (A-C) The sulphotransferase reaction was carried out with chondroitin as the acceptor substrate under conditions described in the Materials and Methods with constructs containing C6ST (A), His-C6ST (B) and His-LacZ (C). The ^{35}S-labelled product was digested with chondroitinase ACII (△) or chondroitinase ACII + chondro-6-*O*-sulphatase (*). The digests were subjected to Partisil-10 SAX HPLC and eluted fractions were monitored for radioactivity. Arrows indicate elution positions of standard disaccharides: (1) 2-acetamide-2-deoxy-3-*O*-(β-D-gluco-4-enepyranosyluronic acid)-D-galactose (ΔDi-0S); (2) 2-acetamide-2-deoxy-3-*O*-(β-D-gluco-4-enepyranosyluronic acid)-6-*O*-sulpho-D-galactose (ΔDi-6S); (3) 2-acetamide-2-deoxy-3-*O*-(β-D-gluco-4-enepyranosyluronic acid)-4-*O*-sulpho-D-galactose (ΔDi-4S); (4) inorganic sulphate; and (5) 2-acetamide-2-deoxy-3-*O*-(β-D-gluco-4-enepyranosyluronic acid)-4,6-bis-*O*-sulpho-D-galactose (ΔDi-diS_E). The broken line depicts the eluting salt gradient.

Sulphation of chondroitin by the recombinant rat C6ST-1

To confirm that the rat cDNA encodes a protein with C6ST activity, the sequence was expressed in COS-7 cells. We generated two different expression constructs, pcDNA-C6ST-1 containing the full-length *C6st1*, and pcDNA-His-C6ST-1 lacking the N-terminal transmembrane domain but retaining the PAPS-binding sites and the catalytic domain. When

Table 1. Overexpression of *C6st1* in COS-7 cells

Plasmid	Sulphotransferase activity (pmol/hour/mg protein)
(i) pcDNA-C6ST-1	13.36±1.23
(ii) pcDNA-His-C6ST-1	12.53±0.91
(iii) pcDNA-His-LacZ	0.58±0.12

COS 7 cells were transfected with an expression plasmid containing either (i) the complete coding sequence of C6ST-1 (pcDNA-C6ST-1), (ii) a truncated C6ST-1 sequence fused to the sequence that encodes $(His)_6$ (pcDNA-His-C6ST-1), or (iii) the pcDNA vector alone. Cell homogenates were assessed for sulphotransferase activity with the use of PAP[^{35}S] as donor and chondroitin as acceptor; the yield of ΔDi-6[^{35}S] after digestion of the product with chondroitinase ACII was determined. Values represent mean ± s.d. of triplicate cultures.

transfected into COS-7 cells, both constructs yielded products that indicated similar sulphotransferase activity in an in vitro assay with chondroitin as acceptor. The activities were at least 20-fold greater than that of control transfectants bearing pcDNA-His-LacZ (Table 1). This confirmed that the expressed product of the cloned cDNA possessed sulphotransferase activity.

To determine whether the sulphotransferase assay succeeded in the transfer of sulphate from PAP[^{35}S] to C-6 of GalNAc residues of chondroitin, the ^{35}S-labelled products were digested with chondroitinase ACII to yield disaccharides that were then analyzed with the use of Partisil-10 SAX HPLC (Fig. 1). A single ^{35}S-labelled peak (peak 2 in Fig. 1A,B) that corresponded to reference ΔDi-6S was observed. Further digestion of the labelled disaccharide with chondro-6-sulphatase resulted in a shift of the radioactive peak to an elution position that corresponded to inorganic [^{35}S]sulphate. This was observed in both test transfectants that carried either pcDNA-C6ST-1 (Fig. 1A) or pcDNA-His-C6ST-1 (Fig. 1B) but not in control transfectants that carried pcDNA-His-LacZ (Fig. 1C). These results confirmed that C6ST-1 catalyzed the transfer of sulphate only to C-6 of GalNAc residues of repeating disaccharide units of chondroitin.

Upregulated *C6st1* mRNA in Schwann cells that emigrate from sciatic nerve explants

To study *C6st1*-expressing cells derived from the nerve away from hematogenous infiltrates and axonal sprouts, we cultured explants of adult rat sciatic nerve segments where severed axons had degenerated and compared these with confluent cultures of purified Schwann cells. Schwann cells that migrated out of the sciatic nerve explants showed intense CS56 immunopositivity (Fig. 2A), contrasting with the barely visible CS56 immunopositivity of Schwann cells in confluent cultures (Fig. 2B). This suggests that CSPGs are produced in association with Schwann cell emigration from the nerve explants and that the chondroitin moieties are enriched in tetrasaccharide motifs (Ito et al., 2005) of 4-sulphated disaccharide linked to 2,6-bissulphated disaccharide as recognised by the monoclonal antibody CS56. The proportion of Schwann cells expressing the *C6st1* transcript was also significantly higher among those exiting from sciatic nerve explants than those in confluent cultures (41.1±5.2% versus 7.1±2.9%, P<0.001; Fig. 2C). Taken together, the results indicate that under in vitro conditions that allow migration of cells out of explants, migratory Schwann cells upregulate

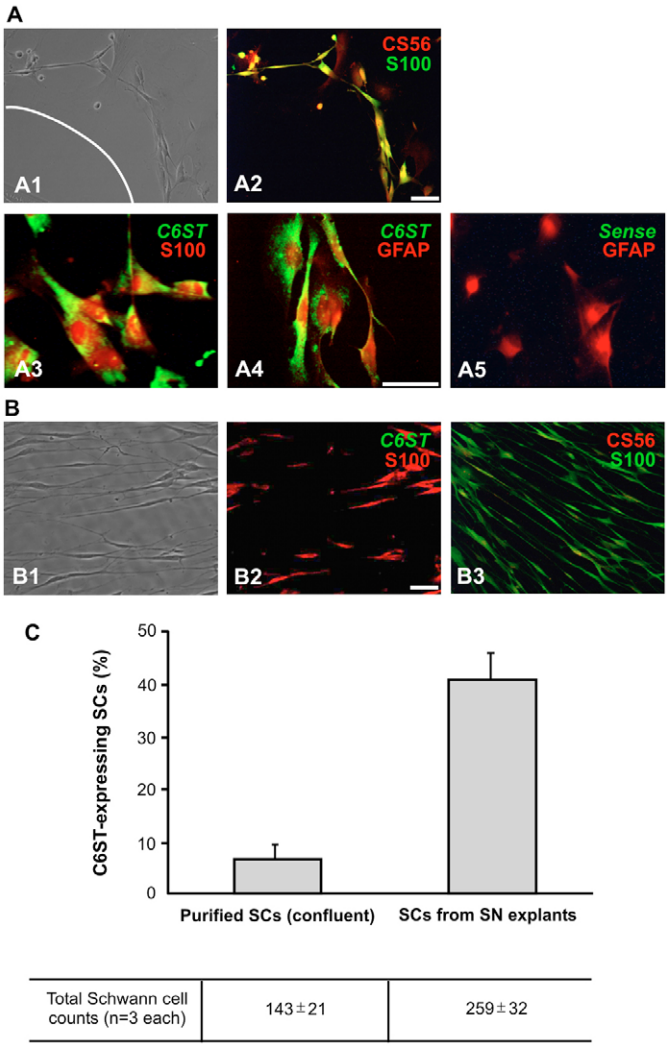

Fig. 2. *C6st1* mRNA expression is upregulated in Schwann cells emigrating from sciatic nerve explants but not in Schwann cells at confluence. Schwann cells emigrating from explants of sciatic nerves (adult rats) are compared with confluent cultures of purified Schwann cells. (A) Phase-contrast (A_1) and immunofluorescence (A_2) views of emigrating Schwann cells doubly immunopositive for the S100 and CS56 epitopes. Emigrating Schwann cells reveal colocalisation of fluorescence in situ hybridisation signal for *C6st1* mRNA (*C6ST*) and immunofluorescence for either S100 (A_3) or GFAP (A_4). The GFAP-positive migrating Schwann cells show negligible hybridisation signal when tested with the sense riboprobe (A_5). (B) Phase-contrast (B_1) and combined hybridisation- and immunofluorescence (B_2) views of confluent cultures of purified Schwann cells, showing insignificant expression of *C6st1* mRNA in spindle-shaped, bipolar, S100-positive Schwann cells. Similarly, these Schwann cells were S100-positive but CS56-negative, as observed with double immunofluorescence (B_3). (C) Histogram showing prevalence of C6ST-expressing, S100-positive Schwann cells (SC) in the sciatic nerve (SN) explant over those in confluent cultures of purified Schwann cells (P<0.001). Total Schwann cell counts are listed under the histogram. Error bars represent s.e.m. of three independent experiments. Bars, 25 μm (B, upper panels in A); 50 μm (lower panels in A).

C6st1 expression and that these cells produce chondroitin moieties bearing CS56 epitopes.

Downregulated *C6st1* mRNA in Schwann cells that engage in interactions with axon networks

To find if migrating Schwann cells modulate *C6st1* expression in the presence of growing axons, DRG explants of E15 rats were studied in culture. We found expression of *C6st1* transcripts in Schwann cells that populated the migration front, sometimes ahead of axonal arbors (Fig. 3B). Time-lapse video microscopy revealed frequent changes in shape and mobility ranges of up to 2 μm/minute among Schwann cells at the frontier (950-1400 μm from the DRG centre). They frequently but transiently contacted axonal arbors and changed axonal contacts along the way (supplementary material Movie 1 and Fig. S2). Occasionally, the Schwann cells made strides of ⩾2 μm/minute with lamellipodial extensions in the forward direction followed by tail retraction. Expression reached barely detectable levels among Schwann cells that lagged behind and became engaged with axonal fascicles (Fig. 3A-C; supplementary material Fig. S2). Evidence is thus provided not only for the expression of *C6st1* in migrating Schwann cells but also for downregulated expression in Schwann cells that became limited in mobility and committed to interactions with axons.

Changes in Schwann cell motility with chondroitinase ABC treatment of DRG cultures

If C6ST-expressing Schwann cells at the frontier were secreting 6-sulphated chondroitin products to modulate motility, we proposed that digestive removal of these moieties would affect Schwann cell motility. To test this, DRG cultures were pre-treated for an extended period (40 hours) with chondroitinase ABC. Enzyme-treated cultures revealed 3B3 immunopositivity about S100-positive Schwann cells at the migration front (Fig. 4A-D), whereas control treatment showed no 3B3 immunoreactivity (Fig. 4E-H). The stubs of 6-sulphated disaccharides of chondroitin, detectable by 3B3 immunoreactivity (Caterson et al., 1984), provide not only evidence for the action of chondroitinase ABC on CSPGs, but also proof of the concept that proteoglycans bearing 6-sulphated chondroitin moieties were secreted into the pericellular environment of Schwann cells at the frontier. Parallel cultures were studied with time-lapse video microscopy. Motility analysis of Schwann cells revealed a general shift to wide-range motilities of 0-4.6 μm/minute following chondroitinase ABC treatment (compare Figs S2 and S3 in supplementary material). This suggests that the majority of chondroitin sulphate moieties pre-existing in the environment of the DRG explant cultures limited Schwann cell motility. This does not necessarily reflect the property of chondroitin sulphate moieties freshly produced by migrating Schwann cells. To demonstrate effects of chondroitin sulphate moieties freshly produced by Schwann cells actively migrating in the frontier, cultures were pre-digested of existing matrix chondroitin sulphate (16 hours) with chondroitinase ABC. Cultures were then paired, one with enzyme treatment during 3 hours of time-lapse video recording versus another with omission of enzyme in control treatment for the same period, for the comparison of Schwann cell motility. Results of these experiments indicated that Schwann cells at the frontier tended to decline in motility with the 3-hour enzyme treatment: a decrease from 30% to 16% of mapped Schwann cells falling within the high-motility range (⩾50% of steps exceeding

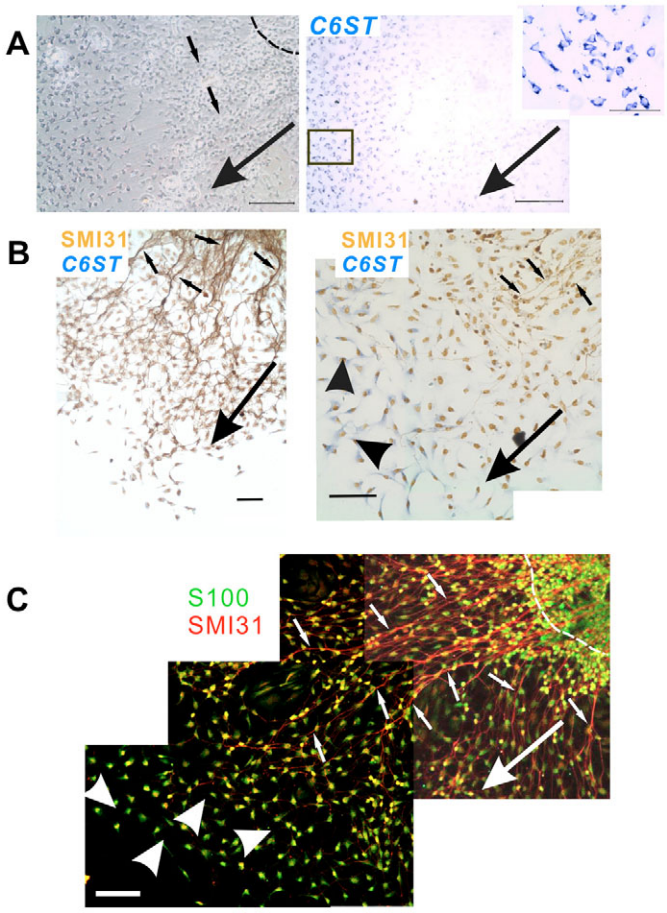

Fig. 3. *C6st1* mRNA expression is upregulated in migrating Schwann cells and not in Schwann cells that are engaged with axonal fascicles. DRG explants (E14 rats) were cultured on laminin-coated coverslips for 2 days in 10% FBS-DMEM-F12 supplemented with NGF (20 ng/ml). (A) Left panel, phase-contrast view of axons (small arrows) and cells radiating from the explant. Right panel, the same view showing *C6st1* mRNA (*C6ST*) hybridisation signals in cells at the frontier (box); the enlarged inset image of the boxed region reveals the various morphologies of *C6st1*-expressing cells. (B) In situ hybridisation for *C6st1* mRNA combined with SMI31 immunocytochemistry for axons. Left panel, SMI31-positive fibres (small arrows) radiate as networks and fascicles from a DRG explant. *C6st1* hybridisation signals were hardly visible in cells associated with axonal fascicles. Towards the frontier (⩾1090 μm from DRG centre), *C6st1*-expressing were visible. Right panel, an enlarged view of the frontier zone shows scattered *C6st1*-expressing cells (arrowheads) apparently in advance of SMI31-positive axons (small arrows). (C) Double immunofluorescence for SMI31-positive axons and S100-positive Schwann cells. S100-positive cells can be seen crowded around the DRG explant (upper right), aligned as chains along SMI31-positive axon fascicles (small arrows), and as scattered cells (arrowheads) in the frontier. The large arrow in each panel indicates the direction of projection of growing axons and emigrating cells from the DRG centre. Bars, 200 μm (A,B), 100 μm (C).

2.3 μm/minute; Fig. 4I) and an increase from 20% to 43% of mapped Schwann cells falling within the low-motility range (⩾50% of steps lower than 1.5 μm/minute, Fig. 4I). In situ hybridisation for *C6st1* mRNA in cultures fixed after the live-cell imaging confirmed expression among the Schwann cells

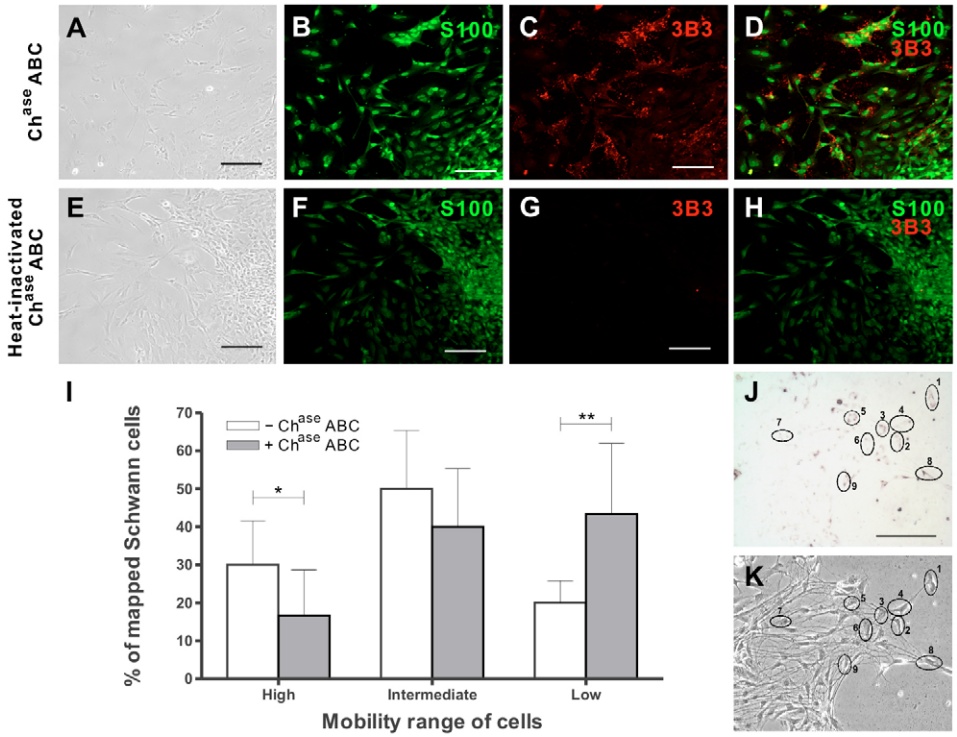

Fig. 4. Chondroitinase digestion of pericellular proteoglycans of migrating Schwann cells at the DRG frontier results in a shift to lower mobilities. (A-D) Extended treatment with chondroitinase ABC (40 hours) revealed cells radiating from the DRG centre (towards lower right, phase-contrast view in A), many of which were S100-positive Schwann cells (B) bearing pericellular 3B3-immunopositivity (C). (D) Merged image of B and C. (E-H) Although control treatment with the heat-inactivated enzyme similarly revealed cells radiating from the DRG centre (towards mid-right, phase-contrast view in E), none of the S100-positive cells (F) showed pericellular 3B3-immunopositivity (G). (H) Merged image of F and G. The bar chart (I) shows the shift towards lower mobility among Schwann cells at the migration front during time-lapse video recording of cultures undergoing a further 3-hour treatment with (+) chondroitinase ABC compared with those without (–) the enzyme. Mobility ranges are classified high at >2.3 μm/minute, intermediate at 1.5-2.3 μm/minute and low at <1.5 μm/minute. Results are the mean ± s.e.m. of triplicate DRG experiments prepared for time-lapse video recording (*P=0.46; **P=0.29). (J,K) One of these DRGs is shown both under light microscopy to reveal *C6st1* mRNA signals (J) and under phase-contrast optics to reveal cell profiles (K). Cells that had been mapped for mobility measurements were numbered as indicated. The corresponding video clip and profile of cell mobility are shown in supplementary material Movie 2 and Fig. S3. Bars, 100 μm (A-H) and (J,K).

mapped for motility assessment (Fig. 4J,K). Given the inherent heterogeneity in sulphation of the chondroitins, the results suggest that chondroitin moieties produced by *C6st1*-expressing Schwann cells at the frontier of the 3-hour live-cell observation are sufficient to facilitate migration of Schwann cells at the frontier.

Upregulated *C6st1* mRNA in GFAP-positive Schwann cells in an early phase of tissue reorganisation after nerve crush

To examine whether the mobile Schwann cells in vivo also upregulate *C6st1* expression, sections of the sciatic nerves at indicated stages after injury were hybridised with the anti-sense riboprobe for *C6st1*. Progressively intensifying signals were observed in the cytoplasm of Schwann cells that initially took the form of annulae around as yet undetectable myelin within 1 day post crush (dpc) (Fig. 5A) and expanded to various shapes that filled the Bands of Büngner by 3-7 dpc (Fig. 5A). During this time, the injured axons degenerated distal to the injury and Schwann cells were mobile to scavenge myelin and axonal debris. By 14 dpc, the signals condensed and returned to the annular morphology about regrowing axons (Fig. 5A). Day 28 post crush nerves indicated barely detectable *C6st1* expression, similar to that observed in normal nerves (Fig. 5A). The hybridisation patterns revealed with the antisense riboprobe were clearly different from those revealed with the sense riboprobe, as exemplified by the section of 14 dpc sciatic nerves (Fig. 5A). The results support a wave of upregulated *C6st1* expression in association with Schwann tube reorganisation after crush injury.

To provide further evidence that upregulated *C6st1* expression was indeed in a mobile subset of Schwann cells, sections of 7 dpc sciatic nerves were subjected to in situ hybridisation for *C6st1* mRNA and further immunostained for markers of Schwann cells, S100 (expressed in both non-myelinating and myelinating Schwann cells) or GFAP (expressed in non-myelinating Schwann cells and reversibly suppressed in myelinating Schwann cells) (Jessen et al., 1990; Jessen and Mirsky, 2005) (Fig. 6). The merged images indicated that not all S100-positive cells expressed *C6st1* mRNA (Fig. 6C,G) but all *C6st1*-expressing cells showed GFAP immunopositivity (Fig. 6K,O). The results indicate that a sub-population of Schwann cells that reacted to the injury with GFAP expression upregulated synthesis of C6ST-1. Although ED-1-positive macrophages recruited to the injured site were identifiable in the tissue sections, only a few of the ED-1-positive cells indicated *C6st1* mRNA expression. Perivascular, epineurial and perineurial fibroblasts indicated expression of *C6st1* mRNA similar to those in uninjured tissues. Expression of *C6st1* was therefore upregulated mainly in the sub-population of Schwann cells that reacted to the injury with GFAP expression.

Alternative evidence of early *C6st1* mRNA expression in the crushed sciatic nerve was obtained from RT-PCR analysis that targeted a 675 bp fragment of the rat *C6st1* (427-1101 bp, GenBank AF178689). Signals of the target C6ST-1 sequence relative to that of the reference GAPDH were increased as early

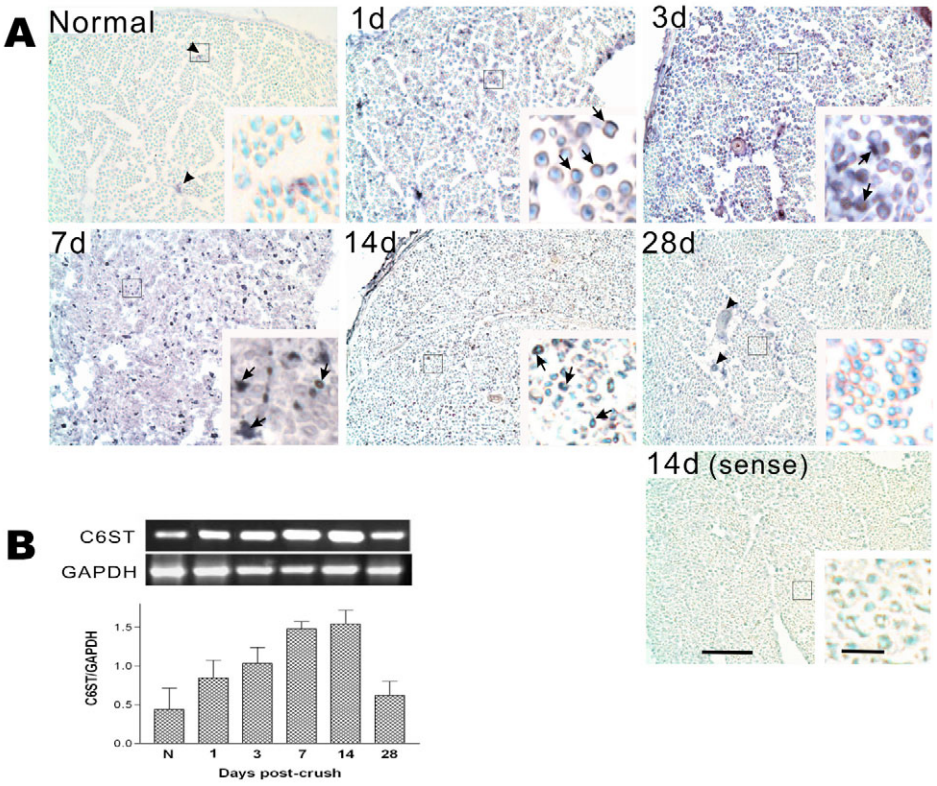

Fig. 5. Upregulated *C6st1* mRNA in Schwann cells during an early phase of tissue reorganisation after nerve crush. (A) In situ hybridisation patterns of *C6st1* mRNA revealed with DIG-labelled antisense probes on transverse cryosections of normal and post-crush sciatic nerves (at 1, 3, 7, 14 and 28 days as indicated). Arrows in the zoom views (insets) indicate significant *C6st1* transcripts in cells circumferential to axons (1 dpc), in irregularly shaped cells profusely distributed about Schwann tubes undergoing reorganisation (3 dpc and 7 dpc). By 14 days post crush, signals were detectable only in the small-diameter Schwann tubes. Signals approach the normal pattern by 28 dpc. Occasional *C6st1* transcripts are detectable around blood vessels (arrowheads in normal and 28-day images). The DIG-labelled sense probe yielded negligible hybridisation signal against the background as exemplified with a section of a 14 dpc sciatic nerve. (B) RT-PCR analysis of *C6st1* mRNA expression for the profile of change in post-crush sciatic nerves (days 1-28 as indicated) against the expression of GAPDH as an internal reference. Gel bands are shown directly above the corresponding histogram of C6ST: GAPDH intensity ratio. Results are the mean ± s.e.m. of three independent sets of analyses. Bars, 200 μm.

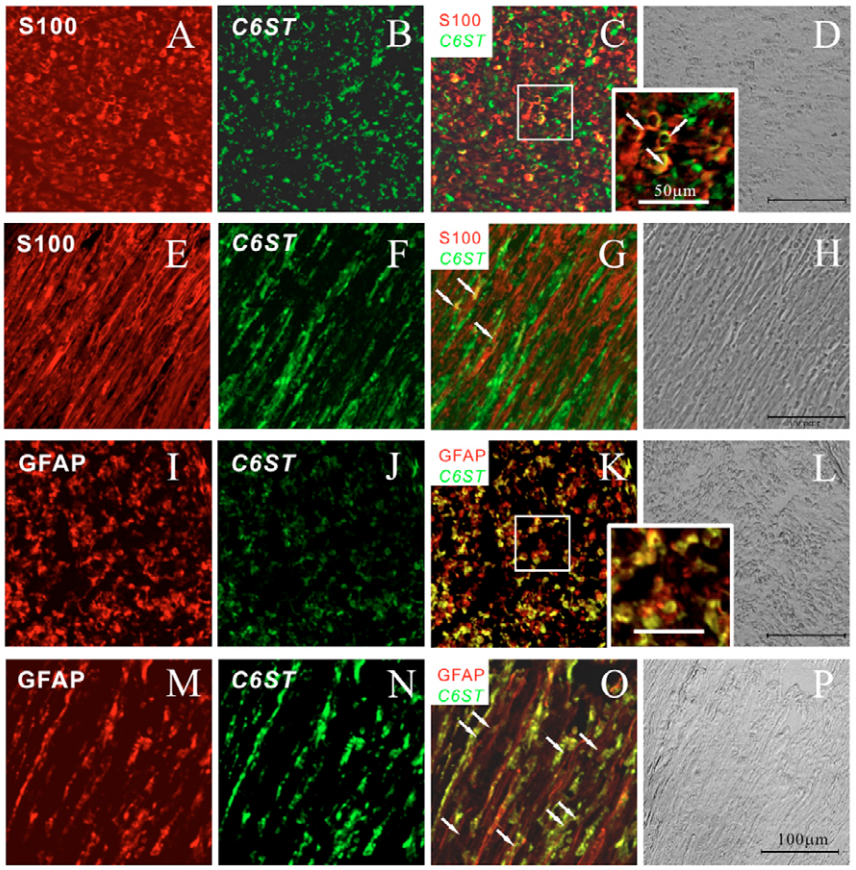

Fig. 6. Expression of *C6st1* mRNA in Schwann cells in 7 dpc nerves. Fluorescence in situ hybridisation for *C6st1* mRNA in combination with fluorescence immunohistochemistry for either S100 (A-H) or GFAP (I-P). Images represent both transverse (A-D and I-L) and longitudinal (E-H and M-P) cryosections of 7 dpc sciatic nerves at the crush site. Phase-contrast views of the tissues are shown in the right-hand column. Merges of immunocytochemistry and hybridisation images are shown (C,G,K and O) with enlarged views (insets) of the boxed areas (C and K). Only some of the S100-positive Schwann cells expressed the *C6st1* transcript (arrows) but all *C6st1*-expressing Schwann cells were GFAP-positive. Bars, 100 μm (A-P); 50 μm (insets).

as 1 dpc and remained high up to 14 dpc. This contrasts with ratios indicated by nerves at 28 dpc or normal nerves (Fig. 5B) in which Schwann cell motility is expected to be low. The results support the notion of upregulated *C6st1* expression in an early phase of tissue reorganisation after sciatic nerve crush.

Discussion

In this first report of *C6st1* expression in migratory Schwann cells, we followed up the evidence of increased 6-sulphated chondroitins in crushed sciatic nerves and cloned the cDNA of the rat *C6st1*. With riboprobes generated against the rat *C6st1* sequence, we found upregulated expression in Schwann cells that assumed migratory phenotypes during an early phase of tissue reorganisation after sciatic nerve crush. Expression returned to basal levels when Schwann cells resumed association with axons as in the myelinating phenotype. In cultures of sciatic nerve segments where severed axons have degenerated, *C6st1* expression among migrating Schwann cells was independent of axons. To observe Schwann cells and growing axons in action, we successfully used cultures of embryonic DRG and staged treatment of the cultures with chondroitinase ABC to provide new insight to the dynamics of *C6st1*-expressing Schwann cells at the migration front where they make transient contacts with axonal arbors along the way. This contrasts with undetectable *C6st1* expression among Schwann cells that remain persistently with axonal fascicles.

Although increased chondroitin sulphates have been reported in injured peripheral nerves (Shum and Chau, 1996; Zuo et al., 1998), the fact that these are mainly soluble and extracellular has left the cellular source of the various sulphated chondroitin isoforms unclear. Attempts to target the core proteins of CSPGs found immunopositivities associated with non-neuronal elements of peripheral nerves – Schwann cells, perineurial and endoneurial fibroblasts, and blood vessels (Braunewell et al., 1995; Martin et al., 2001; Schneider et al., 2001; Rezajooi et al., 2004), but these at best indicated where the secreted or shed CSPGs were deposited. Little is known about the sulphated glycoforms on site or at source. In the injured sciatic nerve, biochemical analyses revealed a distinctive increase in 6-sulphated chondroitin isoforms (Braunewell et al., 1995; Chau and Shum, 1997). This change followed a time course coincident with tissue reorganisation towards nerve regeneration. This led us to find *C6st1* expression in migratory cells and to determine whether expression persists when the migratory cells associate with regrowing axons.

In this study, we found upregulated expression of *C6st1* mRNA in an early phase of tissue re-organisation after nerve injury. Although *C6st1* signals were identifiable in perivascular, perineurial and endoneurial fibroblasts of crushed nerves, expression in these cell types did not differ significantly from those in uninjured sciatic nerves. By contrast, a significant increase in *C6st1* signals was found in Schwann cells that changed from quiescent, myelinating cells in the uninjured nerve into various forms in the reorganising Schwann tubes of the crushed sciatic nerve. One early reaction of myelinating Schwann cells to the loss of contact with axons involves transformation to myelin-phagocytosing cells (Hirata et al., 2000). Another possibly related immediate response involves the release of galectin-1 from damaged axons and Schwann cells (Fukuya et al., 2003). Injury-induced production of nitric oxide into the extracellular environment mediates conversion of galectin-1 to the oxidised form (Levy et al., 2000). Given that oxidised galectin-1 stimulated peritoneal macrophages to produce soluble factors that promoted Schwann cell migration in vitro (Horie et al., 2004), injury-induced activation of resident, endoneurial macrophages in vivo (Mueller et al., 2001) could likewise facilitate the conversion of myelinating Schwann cells to a mobile phenotype that scavenges myelin debris. In the present study, we further found GFAP-positive Schwann cells upregulated in *C6st1* expression in the crushed nerve. GFAP expression is characteristic of both immature and non-myelinating Schwann cells (Jessen et al., 1990; Jessen and Mirsky, 2005) and is recapitulated as early as 24 hours after nerve injury (Cheng and Zochodne, 2002). Given an association of GFAP expression with Schwann cell motility, we suggest that enzymatic activity of the upregulated *C6st1* yields 6-sulphated chondroitin products that modulate adhesion of Schwann cells to the basal lamina in coordination with the increased cell motility.

Our in vitro observations reinforce this suggestion. With cultures of sciatic nerve segments, migrating Schwann cells removed from axonal influence were clearly distinguishable by expression of GFAP and *C6st1*. With cultures of embryonic DRG explants treated in stages with chondroitinase ABC, we were able to decipher facilitatory effects of chondroitin sulphate moieties on the motility of Schwann cells at the migration front during 3 hours of time-lapse video recording. Not only were these Schwann cells distinguishable by *C6st1* mRNA expression, products of the C6ST activity were identifiable as 3B3-immunopositivity in their pericellular environment. These Schwann cells apparently sustained axonal growth through frequent neurotrophic contacts with arborisations at the frontier. The shape changes of these Schwann cells also suggest dynamic renewal of pericellular 6-sulphated chondroitin moieties. Given that the 6-sulphated chondroitin moieties have not entered states of aggregation characteristic of those in the extracellular matrix, there is implication for their involvement in transient destabilisation of cell adhesion to the substratum or in trophic interactions with axonal arbors.

As Schwann cells migrate ahead, we expect a trail of CSPG deposits that represent various states of aggregation with matrix molecules. Both electron microscopy and computer modelling of chondroitin sulphate isomers have shown that 6-sulphated chains assume a secondary structure that can electrostatically and sterically accommodate close packing of 6-sulphated and non-sulphated chondroitins but not 4-sulphated chondroitins (Scott et al., 1992). The capacity for aggregation among 6-sulphated chondroitins and non-sulphated glycosaminoglycans such as hyaluronans (Turley and Roth, 1980; Scott, 2003) suggests a matrix that is not readily penetrable by advancing terminals of growing axons. Neuritic outgrowths that do pioneer through a matrix dominated by aggregating glycosaminoglycans and proteoglycans will necessarily provide the scaffold to which follower outgrowths can fasciculate. Fasciculation has indeed been shown in the guidance of axons through an environment of aggregating CSPGs (Snow et al., 2003). In DRG explants, we also observed fasciculated neurites in regions where neurite outgrowth navigated through a matrix deposited by *C6st1*-expressing, migratory Schwann cells.

In addition to *C6st1*-expressing Schwann cells that emigrated free from each other, we found low-to-negligible *C6st1* expression among Schwann cells that were committed to engagement with axonal fascicles as evident in cultures of embryonic DRG explants. This latter is consistent with the low chondroitin sulphate expression that we found in confluent cultures of purified Schwann cells. These Schwann cells turned out to participate in axon ensheathment and myelination in nerve-bridging channels that guide axonal regrowth across injured nerve stumps, not only in the sciatic nerve but also in the spinal cord (Chau et al., 1999; Chau et al., 2004; Bunge, 2001). The pericellular environment of low *C6st1*-expressing Schwann cells are therefore amenable to sustained cellular contact and Schwann cell-guided axonal growth.

Overall, these observations reveal 6-sulphation of chondroitins as a mechanism to fine-tune the pericellular environment of Schwann cells both in the developmental programme of the embryonic DRG and in the regenerative programme of the crushed nerve. In both programmes, GFAP-positive Schwann cells are the major cellular source of upregulated *C6st1* that contributes to the production of pericellular 6-sulphated CSPGs. The expression is upregulated in coordination with Schwann cell migration and becomes downregulated when Schwann cells are engaged in interactions with axonal fascicles. Increased 6-sulphated chondroitin domains in the pericellular environment of Schwann cells provide optimum adhesiveness for the mobile phenotype of Schwann cells. Further work will be necessary to understand how the pioneer axons succeed to negotiate through chondroitin sulphate-enriched matrix deposits at different stages.

Materials and Methods

Rats, explants, and Schwann cell culture

Nerve crush was performed on sciatic nerves of pentobarbital-anaesthetised (40 mg/kg body weight) male Sprague Dawley rats (200-250 g) as described (Shum and Chau, 1996). After 1, 3, 7, 14 and 28 days of recovery, animals were sacrificed by decapitation and the sciatic nerves were collected. Sciatic nerves were also collected from uninjured animals as controls. All procedures were in strict accordance with the NIH Guide for the care and use of laboratory animal and approved by the Committee on Use of Live Animals for Teaching and Research, Faculty of Medicine, The University of Hong Kong.

In some cases, sciatic nerves were harvested from uninjured rats for the preparation of Schwann cell cultures (Morrissey et al., 1991). Briefly, nerves were stripped of connective tissue, cut into 1-mm segments, and cultured in 10% FBS-DMEM. When emigrating cells reached confluence, explant tissues were subcultured. The process was repeated four to six times until 99% of cells that emigrated from the explants were Schwann cells. The explants were dissociated with 0.5% collagenase (Sigma, St Louis, MO) in 15% FBS-DMEM (24 hours, 37°C) and then seeded onto poly-L-lysine-coated flasks. Cell proliferation was stimulated by repeated treatment with forskolin (20 μM; Sigma) and pituitary extract (20 μg/ml; Sigma). Cells were then returned to 10% FBS-DMEM and cultured for 7 days before they were subcultured onto poly-L-lysine-coated coverslips.

Dorsal root ganglia were dissected from E15 rats in serum-free medium. Two to three explants were seeded per laminin-coated glass coverslip. Explants were cultured in 10% FBS-DMEM-F12 (Sigma) in four-well plates for 24 hours. On the second day, the culture medium was supplemented with nerve growth factor (NGF; Sigma) at 20 ng/ml and the explants were left in culture for another 24 hours before fixation in 4% (w/v) paraformaldehyde.

cDNA synthesis, RT-PCR and cloning of rat *C6st1*

Total RNA was extracted from rat sciatic nerves by the modified acid-phenol-guanidinium thiocyanate method (Chomczynski and Sacchi, 1987). Oligo-dT-primed first-strand cDNAs were generated from total RNA using the SuperScript II kit (Invitrogen, Carlsbad, CA). PCR amplification of cDNAs was performed using HotstarTaq DNA polymerase (Qiagen, Germany) and degenerate primers corresponding to conserved sequences of known human, mouse and chick C6ST genes: sense primer for full-length *C6ST-1* (C6ST-F-s), 5′-CCATGGAG-AAAGGACTCRCTTTG-3′; antisense primer for full-length *C6ST-1*, (C6ST-F-as), 5′-CTACGTGACCCAGAAGGTGCC-3′; sense primer for partial *C6ST-1* (C6ST-P-s), 5′-TTCGTKGGSGAGTTCTTCAAC-3′; and antisense primer for partial *C6ST-1* (C6ST-P-as), 5′-CTCATAGCGCACCARCATGT-3′. The latter amplified a 675 bp fragment corresponding to the high homology sequence of *C6st1* (427-1101 bp, GenBank AF178689). As a reference, an 843 bp fragment of GAPDH cDNA was amplified, using primers: 5′-CCTTCATTGACCTCAACTACATGGT-3′ and 5′-TCATTGTTATACCAGGAAATGAGCT-3′.

The partial sequence of *C6st1* was amplified with PCR initiated at 95°C (15 minutes), followed by 36 cycles at 94°C (50 seconds), 58°C (1 minute), 72°C (1 minute) and terminated at 72°C (7 minutes). The full coding sequence of rat *C6ST* was amplified with touch-down PCR, starting with four cycles at 94°C (50 seconds), 60°C (1 minute) and 72°C (1 minute), followed by decreasing annealing temperature by 3°C for every four cycles and finally 25 cycles at 94°C (50 seconds), 50°C (1 minute) and 72°C (1 minute).

The full-length *C6st1* was cloned into pGEM-T-Easy vector (Promega, Madison, WI) and checked with sequencing (ABI 373A automatic sequencer, Applied Biosystems). The nucleotide sequence and corresponding amino acid sequence were analyzed in the ExPASy Proteomics server (Swiss Institute of Bioinformatics). Sequence alignment with published C6ST-1 sequences was performed with the use of Clustal W software.

Transient expression of *C6st1* in COS-7 cells

A truncated *C6st1* cDNA (Bases 142-1425, GenBank accession no. AF178689) lacking the first 47 amino acids at the N-terminal was amplified from pGEM-C6ST-1 and inserted into the expression vector pcDNA-HisA (Invitrogen, Carlsbad, CA) to yield pcDNA-His-C6ST-1. The full coding sequence of C6ST-1 was also subcloned into pcDNA3.1 to result in pcDNA-C6ST-1.

Both recombinant plasmids were transfected into COS-7 cells using FuGENE 6 Transfection Reagent (Roche Molecular Biochemicals, Indianapolis, IN) as recommended by the manufacturer. Briefly, COS-7 cells (5.6×10^6 cells/10 cm dish) were transfected with the relevant plasmids (4 μg). After 65 hours of culture in 10% FCS-DMEM, the cells were washed and then homogenised in 0.25M sucrose, 20 mM Tris-HCl (pH 7.2), 0.5% Triton X-100. The homogenate was centrifuged (10,000 ***g***, 15 minutes, 4°C) and the supernatant was kept as the cell extract.

Assay of sulphotransferase activity

Sulphotransferase activity was assayed using chondroitin as acceptor. The assay mixture contained 50 mM imidazole-HCl (pH 6.8), 1.25 μg protamine chloride, 2 mM oDTT, 5 mM $MnCl_2$, 2 mM ATP, 5 μg chondroitin (Seikagaku, Japan), 1 μM [^{35}S]3′-phosphoadenosine 5′-phosphosulphate (PAPS) (about 5×10^5 cpm, PerkinElmer Life Sciences, Boston, MA), and 10 μl of the cell extract in a final volume of 50 μl. The mixture was incubated at 37°C for 2 hours and then mixed with four volumes of ethanol-potassium chloride (1.3%) to stop the sulphotransferase reaction. ^{35}S-labelled chondroitin products were separated from [^{35}S]PAPS by centrifugation followed by gel filtration in a HiTrap desalting column (Amersham Biosciences, Uppsala, Sweden) and eluted fractions were monitored for radioactivity with liquid scintillation counting (LS6500; Beckman Coulter, Fullerton, CA).

The remaining ^{35}S-labelled chondroitins in the eluates were precipitated with four volumes of absolute ethanol (4°C, 16 hours) and centrifuged at 12,000 ***g*** (5 minutes, 4°C). Each pellet was redissolved in 20 μl Milli-Q water and digested with chondroitinase ACII (100 mU, Seikagaku, Japan) with or without chondro-6-sulphatase (50 mU, Seikagaku, Japan) at 37°C for 15 hours. Disaccharide products were analyzed by chromatography in a Partisil-10 SAX column (Whatman, UK) (Shum et al., 1999).

Time-lapse video microscopy

DRG explants were cultured on laminin-coated μ-slides (Ibidi, Munich, Germany) and maintained in 10% FBS-DMEM-F12 supplemented with NGF (20 ng/ml) at 37°C as described under explant culture. In some cases, cultures were pre-treated with chondroitinase ABC (10 mU/ml, 37°C, 16 hours) before time-lapse video capture on day 2 of culture. The enzyme-treated cultures were then paired – one was incubated with a fresh dose of chondroitinase ABC and the other was incubated without the enzyme. Phase-contrast images of cell movement in the migration front were captured with a Spot 4.2 digital camera connected to an Olympus IX71 light microscope at 3-minute intervals for 180 minutes. The mobility profile of any selected Schwann cell was determined as the displacement of the cell nucleus per 9-minute step over 180 minutes of video recording.

In situ hybridisation

Sciatic nerves were fixed in 4% (w/v) paraformaldehyde for at least 12 hours before cryoprotection with 30% (w/v) sucrose in PBS at 4°C for 6-10 hours. Cryosections (10 μm) were thaw-mounted on SuperFrost® glass slides (Menzel-Glaeser, Germany) and air-dried. Digoxigenin (DIG)-UTP labelled RNA probes (1.4 kb) were transcribed from pGEM-C6ST-1 with the use of a DIG RNA Labeling Kit (SP6/T7, Roche Molecular Biochemicals, Mannheim, Germany). In situ hybridisation (ISH) was performed with minor modifications to standard protocols. Briefly, cryosections were prewarmed and treated with 20 μg/ml Proteinase K at 24°C for 10 minutes. After acetylation with 0.25% (v/v) acetic anhydride in 0.1 M

triethanolamine for 10 minutes, sections were washed in PBS and dehydrated. Hybridisation was carried out with 1 μg/ml probe at 55°C, 16 hours. Sections were then washed twice in 2× SSC, 50% formamide (55°C), followed by more stringent washes, twice in 0.2× SSC (55°C), once in 0.1× SSC (55°C) and once more at 24°C, each for 20 minutes. In cases of DRG and sciatic nerve explants, post-fixed tissues were permeabilised with 2 M HCl (24°C, 10 minutes) before proceeding with acetylation.

To enhance signal detection, the TSA™ (Tyramide Signal Amplification) Biotin System (NEN™ Life Science Products, Boston, MA) was applied. Briefly, after stringent washes, the samples were blocked for 30 minutes before incubation for 1 hour with anti-DIG-peroxidase (1:200; Roche Molecular Biochemicals). Samples were then incubated in turn with Biotin Tyramide (1:70; 10 minutes), streptavidin-AP (1:200; 30 minutes). Chromogen was developed by incubation with NBT-BCIP for 10-20 minutes in a dark, humid chamber. Samples were counterstained in 0.25% (w/v) methyl green (5 minutes), dehydrated and mounted in aquamount (BDH, UK). The stained samples were viewed under light microscopy (IX71; Olympus, Japan) and digital images were imported into CorelDRAW to generate the final figures.

Fluorescence in situ hybridisation in combination with immunofluorescence

The ISH procedure was the same as described above, except that in the detection step, streptavidin-AP was replaced by fluorescein-conjugated streptavidin (NEN™ Life Science Products, Boston, MA) at 1:100 dilution. After fluorescence ISH, samples were incubated for 1 hour with anti-glial fibrillary acidic protein (GFAP) (1:100; rabbit IgG; Biomedical Technologies, Stoughton, MA), anti-S100 (1:200, rabbit IgG; DAKO, Denmark) or ED-1 (1:100, mouse IgG; Serotec, Oxford, UK), followed by incubation for 45 min with TRITC-conjugated anti-rabbit or anti-mouse IgG (1:100; ICN, USA). Subsequently, they were mounted with Gel/mount™ (Biomeda, Foster, CA) and examined under a Bio-Rad MRC-1024 confocal system (Hercules, CA) attached to a Zeiss Axiovert 135M microscope.

Immunocytochemistry prior to in situ hybridisation

Since acid treatment in the ISH procedure interfered with immunostaining with SMI-31, the latter was performed before ISH. DRG cultures were incubated with SMI-31 (1:1000, mouse IgG; Sternberger Monoclonals, Lutherville, ML) (1 hour, 24°C) after they had been treated with 1% (v/v) H_2O_2 to quench endogenous horseradish peroxidase activity. The DRGs were then incubated with horseradish peroxidase-linked goat anti-mouse IgG (1:100; Serotec, Oxford, UK) (1 hour, 24°C) and developed in DAB solution (Pierce, Rockford, IL) for 5 minutes. The tissues were washed with phosphate-buffered saline and then subjected to ISH as described above. The stained cultures were viewed by Olympus light microscopy (IX71, Japan).

Double immunofluorescence

Schwann cell cultures were fixed in 4% (w/v) paraformaldehyde, permeabilised with 0.01% (v/v) Triton X-100, and then incubated with anti-S100 (1:100, rabbit IgG; DAKO, Denmark) and CS56 (1:200, mouse IgM; Sigma) (1 hour, 24°C). This was followed by incubation with FITC-conjugated goat anti-rabbit IgG (1:100; Sigma) and TRITC-conjugated goat anti-mouse IgG (1:100; Sigma). Subsequently, they were mounted with Gel/mount™ (Biomeda).

DRG cultures were treated with chondroitinase ABC or the heat-inactivated enzyme as control (10 mU/ml, 40 hours, 37°C) before they were incubated live with monoclonal 3B3 (1:100, mouse IgM, Seikagaku) (45 minutes, 37°C). This was followed with fixation and permeabilisation, incubation with anti-S100 and then the mixture of FITC-conjugated goat anti-rabbit IgG and TRITC-conjugated goat anti-mouse IgG and then mounted with Gel/mount™ as described above.

Viewing and image capture was performed under a Zeiss Axioplan2 microscope equipped with a Sony CCD camera (DKC-ST5, San Diego, CA) or a Bio-Rad MRC-1024 confocal system (Hercules, CA) attached to a Zeiss Axiovert 135M microscope. Image preparation, assembly and analysis were performed in Photoshop 6.01. In all cases, balance and contrast were adjusted for optimal contrast and brightness.

Statistical analysis

Differences between groups were analyzed with the Student's *t*-test (InStat v2.04a program, GraphPad Software) and considered significant at $P<0.05$. All statistical tests were two-tailed.

This work was supported by The Hong Kong Research Grants Council (HKU7294/01M to DKYS). X.L. was supported by a Cheng Yu-Tung Fellowship for his contribution to the work in HKU. We thank Simon S. M. Chan and Alice Y. Y. Lui for excellent technical assistance.

References

Braunewell, K. H., Martini, R., LeBaron, R., Kresse, H., Faissner, A., Schmitz, B. and Schachner, M. (1995). Up-regulation of a chondroitin sulphate epitope during regeneration of mouse sciatic nerve: evidence that the immunoreactive molecules are related to the chondroitin sulphate proteoglycans decorin and versican. *Eur. J. Neurosci.* **7**, 792-804.

Bunge, M. (2001). Bridging areas of injury in the spinal cord. *Neuroscientist* **7**, 325-339.

Caterson, B., Christner, J. E., Baker, J. R., Couchman, J. R. (1985). Production and characterization of monoclonal antibodies directed against connective tissue proteoglycans. *Fed. Proc.* **44**, 386-393.

Chau, C. H. and Shum, D. K. Y. (1997). Injury-associated increase in 6-sulphated chondroitin sulphates in post-crush sciatic nerves of adult guinea pigs. *Glycoconj. J.* **14**, S9.

Chau, C. H., Shum, D. K. Y., Chan, Y. S. and So, K.-F. (1999). Heparan sulphates upregulate regeneration of transected sciatic nerves of adult guinea pigs. *Eur. J. Neurosci.* **11**, 1914-1926.

Chau, C. H., Shum, D. K. Y., Li, H., Pei, J., Lui, Y. Y., Wirthlin, L., Chan, Y. S. and Xu, X.-M. (2004). Chondroitinase ABC enhances axonal regrowth through Schwann cell-seeded guidance channels after spinal cord injury. *FASEB J.* **18**, 194-196.

Cheng, C. and Zochodne, D. W. (2002). In vivo proliferation, migration and phenotypic changes of Schwann cells in the presence of myelinated fibres. *Neuroscience* **115**, 321-329.

Chomczynski, P. and Sacchi, N. (1987). Single-step method of RNA isolation by acid guanidinium thiocyanate-phenol-chloroform extraction. *Anal. Biochem.* **162**, 156-159.

Clark, R. A., Lin, F., Greiling, D., An, J. and Couchman, J. R. (2004). Fibroblast invasive migration into fibronectin/fibrin gels requires a previously uncharacterized dermatan sulphate-CD44 proteoglycan. *J. Invest. Dermatol.* **122**, 266-277.

Clement, A. M., Nadanaka, S., Masayama, K., Mandl, C., Sugahara, K. and Faissner, A. (1998). The DSD-1 carbohydrate epitope depends on sulfation, correlates with chondroitin sulphate D motifs, and is sufficient to promote neurite outgrowth. *J. Biol. Chem.* **273**, 28444-28453.

Deepa, S. S., Umehara, Y., Higashiyama, S., Itoh, N. and Sugahara, K. (2002). Specific interactions of oversulphated chondroitin sulphate E with various heparin-binding growth factors. Implications as a physiological binding partner. *J. Biol. Chem.* **277**, 43707-43716.

Fernaud-Espinosa, I., Nieto-Sampedro, M. and Bovolenta, P. (1996). Developmental distribution of glycosaminoglycans in embryonic rat brain: relationship to axonal tract formation. *J. Neurobiol.* **30**, 410-424.

Fukuta, M., Uchimura, K., Nakashima, K., Kato, M., Kimata, K., Shinomura, T. and Habuchi, O. (1995). Molecular cloning and expression of chick chondrocyte chondroitin 6-sulphotransferase. *J. Biol. Chem.* **270**, 18575-18580.

Fukuta, M., Kobayashi, Y., Uchimura, K., Kimata, K. and Habuchi, O. (1998). Molecular cloning and expression of human chondroitin 6-sulphotransferase. *Biochim. Biophys. Acta* **1399**, 57-61.

Fukuda, M., Hiraoka, N., Akama, T. O. and Fukuda, M. N. (2001). Carbohydrate-modifying sulphotransferases: structure, function, and pathophysiology. *J. Biol. Chem.* **276**, 47747-47750.

Fukuya, K., Hasegawa, M., Mashitani, T., Kadoya, T., Horie, J., Hayashi, Y., Fujisawa, H., Tachimana, O., Kida, S. and Yamashita, J. (2003). Oxidized galectin-1 stimulates the migration of Schwann cells from both proximal and distal stumps of transected nerves and promotes axonal regeneration after peripheral nerve injury. *J. Neuropathol. Exp. Neurol.* **62**, 162-172.

Habuchi, O. (2000). Diversity and functions of glycosaminoglycan sulphotransferases. *Biochim. Biophys. Acta* **1474**, 115-127.

Henke, C. A., Roongta, U., Mickelson, D. J., Knutson, J. R. and McCarthy, J. B. (1996). CD44-related chondroitin sulphate proteoglycan, a cell surface receptor implicated with tumor cell invasion, mediates endothelial cell migration on fibrinogen and invasion into a fibrin matrix. *J. Clin. Invest.* **97**, 2541-2552.

Hirata, K., He, J. W., Kuraoka, A., Omata, Y., Hirata, M., Shariful Islam, A. T., Noguchi, M. and Kawabuchi, M. (2000). Heme oxygenase1 (HSP-32) is induced in myelin-phagocytosing Schwann cells of injured sciatic nerves in the rat. *Eur. J. Neurosci.* **12**, 4147-4152.

Horie, H., Kadoya, T., Hikawa, N., Sango, K., Inoue, H., Takeshita, K., Asawa, R., Hiroi, T., Sato, M., Yoshioka, T. et al. (2004). Oxidized galectin-1 stimulates macrophages to promote axonal regeneration in peripheral nerves after axotomy. *J. Neurosci.* **24**, 1873-1880.

Ito, Y., Hikino, M., Yajima, Y., Mikami, T., Sirko, S., von Holst, A., Faissner, A., Fukui, S. and Sugahara, K. (2005). Structural characterization of the epitopes of the monoclonal antibodies 473HD, CS-56, and MO-225 specific for chondroitin sulfate D-type using the oligosaccharide library. *Glycobiology* **15**, 593-603.

Jessen, K. R. and Mirsky, R. (2005). The origin and development of glial cells in perpheral nerves. *Nat. Rev. Neurosci.* **6**, 671-682.

Jessen, K. R., Morgan, L., Stewart, H. J. and Mirsky, R. (1990). Three markers of adult non-myelin-forming Schwann cells, 217c(Ran-1), A5E3 and GFAP: development and regulation by neuron-Schwann cell interactions. *Development* **109**, 91-103.

Kitagawa, H., Tsutsumi, K., Tone, Y. and Sugahara, K. (1997). Developmental regulation of the sulfation profile of chondroitin sulphate chains in the chicken embryo brain. *J. Biol. Chem.* **272**, 31377-31381.

Kitagawa, H., Fujita, M., Ito, N. and Sugahara, K. (2000). Molecular cloning and expression of a novel chondroitin 6-O-sulphotransferase. *J. Biol. Chem.* **275**, 21075-21080.

Levy, D., Tal, M., Hoke, A. and Zochondne, D. W. (2000). Transient action of the endothelial constitutive nitric oxide synthase (ecNOS) mediates the development of thermal hypersensitivity following peripheral nerve injury. *Eur. J. Neurosci.* **12**, 2323-2332.

Liu, J., Li, X. G., Chau, C. H. and Shum, D. K. Y. (2001). Expression of chondroitin

6-sulphotransferase mRNA and the sulfation product in post-crush sciatic nerves of adult rats. *Soc. Neurosci. Abstract* 257.6.

Lyons, D. A., Pogoda, H.-M., Voas, M. G., Woods, I. G., Diamond, B., Nix, R., Arana, N., Jacobs, J. and Talbot, W. S. (2005). *erbb3* and *erbb2* are essential for Schwann cell migration and myelination in zebrafish. *Curr. Biol*. **15**, 513-524.

Martin, S., Levine, A. K., Chen, Z. J., Ughrin, Y. and Levine, J. M. (2001). Deposition of the NG2 proteoglycan at nodes of Ranvier in the peripheral nervous system. *J. Neurosci.* **21**, 8119-8128.

Morrissey, T. K., Kleitman, N. and Bunge, R. P. (1991). Isolation and functional characterization of Schwann cells derived from adult peripheral nerve. *J. Neurosci*. **11**, 2433-2442.

Mueller, M., Wacker, K., Ringelstein, E. B., Hickey, W. F., Imai, Y. and Keifer, R. (2001). Rapid response of identified resident endoneurial macrophages to nerve injury. *Am. J. Pathol*. **159**, 2187-2197.

Properzi, F., Carulli, D., Asher, R. A., Muir, E., Camargo, L. M., van Kuppevelt, T. H., ten Dam, G. B., Furukawa, Y., Mikami, T., Sugahara, K. et al. (2005). Chondroitin 6-sulphate synthesis is up-regulated in injured CNS, induced by inury-related cytokines and enhnaced in axon-growth inhibitory glia. *Eur. J. Neurosci*. **21**, 378-390.

Prydz, K. and Dalen, K. T. (2000). Synthesis and sorting of proteoglycans. *J. Cell Sci*. **113**, 193-205.

Rezajooi, K., Pavlides, M., Winterbottom, J., Stallcup, W. B., Hamlyn, P. J., Lieberman, A. R. and Anderson, P. N. (2004). NG2 proteoglycan expression in the peripheral nervous system: upregulation following injury and comparison with CNS lesions. *Mol. Cell Neurosci*. **25**, 572-584.

Sandvig, A., Berry, M., Barrett, L. B., Butt, A. and Logan, A. (2004). Myelin-, reactive glia-, and scar-derived CNS axon growth inhibitors: Expression, receptor signaling, and correlation with axon regeneration. *Glia* **46**, 225-251.

Schneider, S., Bosse, F., D'Urso, D., Müller, H. W., Sereda, M. W., Nave, K. A., Neihaus, A., Kempf, T., Schnolzer, M. and Trotter, J. (2001). The AN2 protein is a marker for the Schwann cell lineage expressed by immature and nonmyelinating Schwann cells. *J. Neurosci*. **21**, 920-933.

Scott, J. E. (2003). Elasticity in extracellular matrix 'shape modules' of tendon, cartilage, etc. A sliding proteoglycan-filament model. *J. Physiol*. **553**, 335-343.

Scott, J. E., Chen, Y. and Brass, A. (1992). Secondary and tertiary structures involving chondroitin and chondroitin sulphates in solution, investigated by rotary shadowing/electron microscopy and computer simulation. *Eur. J. Biochem*. **209**, 675-680.

Shum, D. K. Y. and Chau, C. H. (1996). Changes in glycosaminoglycans during regeneration of post-crush sciatic nerves of adult guinea pigs. *J. Neurosci. Res*. **46**, 465-476.

Shum, D. K. Y., Gohel, M. D. and Tam, P. C. (1999). Hyaluronans: crystallization-promoting activity and HPLC analysis of urinary excretion. *J. Am. Soc. Nephrol*. **14**, S397-S403.

Silbert, J. E. and Sugumaran, G. (2002). Biosynthesis of chondroitin/dermatan sulphate. *IUBMB Life* **54**, 177-186.

Silver, J. and Miller, J. H. (2004). Regeneration beyond the glial scar. *Nat. Rev. Neurosci.* **5**, 146-156.

Snow, D. M., Smith, J. D., Cunningham, A. T., McFarlin, J. and Goshorn, E. C. (2003). Neurite elongation on chondroitin sulphate proteoglycans is characterized by axonal fasciculation. *Exp. Neurol*. **182**, 310-321.

Torigoe, K., Tanaka, H. F., Takahashi, A., Awaya, A. and Hashimoto, K. (1996). Basic behavior of migratory Schwann cells in peripheral nerve regeneration. *Exp. Neurol*. **137**, 301-308.

Tseng, C. Y., Hu, G., Ambron, R. T. and Chiu, D. T. (2003). Histologic analysis of Schwann cell migration and peripheral nerve regeneration in the autogenous venous nerve conduit. *J. Reconstr. Microsurg*. **19**, 331-340.

Turley, E. A. and Roth, S. (1980). Interactions between the carbohydrate chains of hyaluronate and chondroitin sulphate. *Nature* **283**, 268-271.

Uchimura, K., Kadomatsu, K., Fan, Q. W., Muramatsu, H., Kurosawa, N., Kaname, T., Yamamura, K., Fukuta, M., Habuchi, O. and Muramatsu, T. (1998). Mouse chondroitin 6-sulphotransferase: molecular cloning, characterization and chromosomal mapping. *Glycobiology* **8**, 489-496.

Uchimura, K., Kadomatsu, K., Nishimura, H., Muramatsu, H., Nakamura, E., Kurosawa, N., Habuchi, O., El-Fasakhany, F. M., Yoshika, Y. and Muramatsu, T. (2002). Functional analysis of the chondroitin 6-sulphotransferase gene in relation to lymphocyte subpopulations, brain development, and over-sulphated chondroitin sulphates. *J. Biol. Chem.* **277**, 1443-1450.

Zuo, J., Hernandez, Y. J. and Muir, D. (1998). Chondroitin sulphate proteoglycan with neurite-inhibiting activity is upregulated following peripheral nerve injury. *J. Neurobiol*. **34**, 41-54.